Altered Lipid Content Inhibits Autophagic Vesicular Fusion

Hiroshi Koga, Susmita Kaushik and Ana Maria Cuervo

SUPPLEMENTAL MATERIAL

Supplementary Figures and Legends

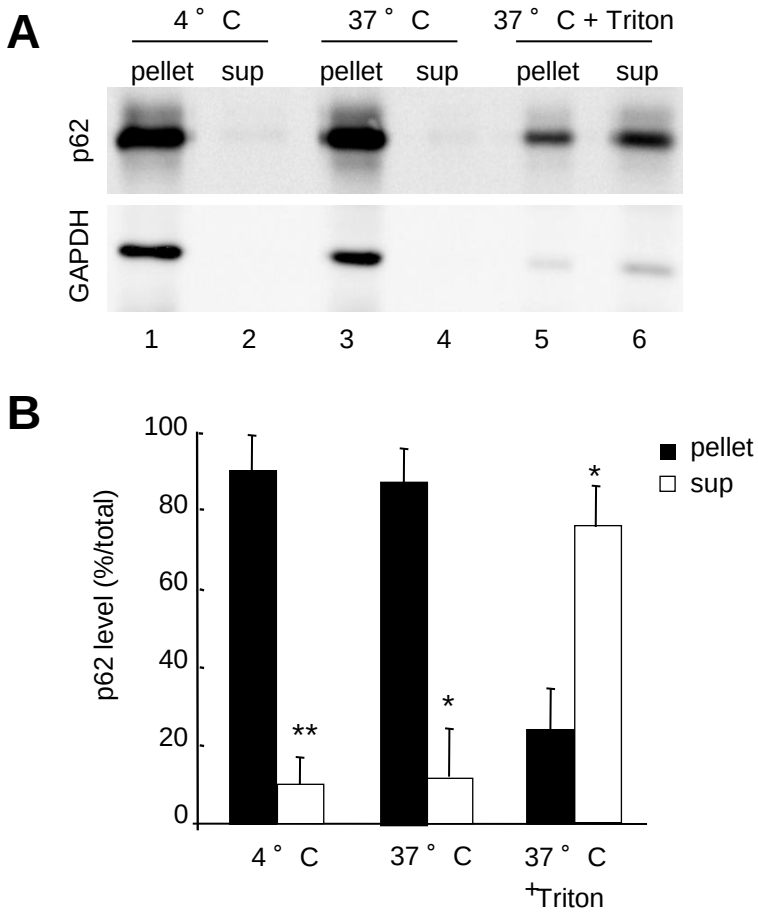

Figure S1. Integrity of isolated autophagosomes. *A)* Autophagosomes (APGs) isolated from starved mice liver were incubated at 4° C or 37° C without additions or in the presence of 0.5% of TritonX-100 for 30 min as labeled. At the end of the incubation, APGs were collected by centrifugation and pellet and supernatant (sup) were subjected to SDS-PAGE and immunoblot for p62 and GAPDH. *B)* The percentage of p62 in each fraction was calculated by densitometric quantification of 3 immunoblots as the one shown in A. Values are expressed as the percentage of p62 present in pellet and supernatant and are mean + S.E. of 3 different experiments. * $P<0.05$.

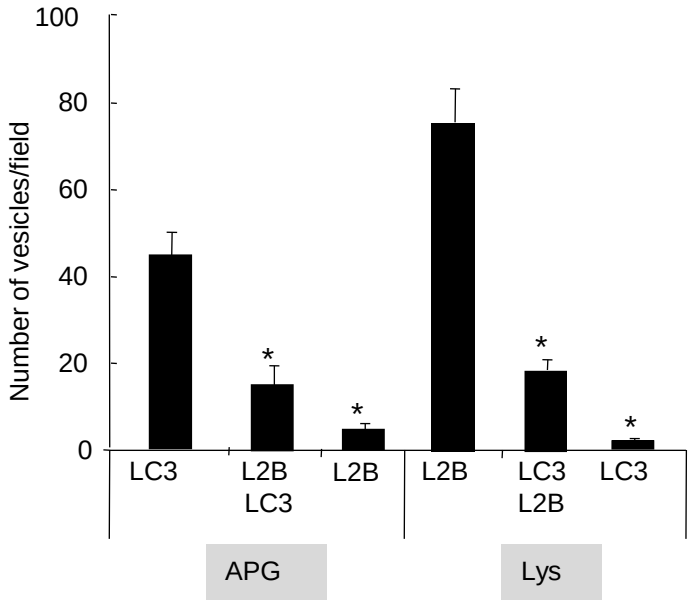

Figure S2. Comparison of labeling of autophagosomes and lysosomes for different markers. Autophagosomes (APGs) and lysosomes (Lys) isolated from starved mouse liver were subjected to immunofluorescence for LC3 and a FITC-conjugated secondary antibody and LAMP-2B and a Cy5-conjugated secondary antibody. Organelles were imaged in the two channels and the number of particles positive for each of the fluorophores and for both of them were quantified. Values are expressed as number of vesicles per microscopic field and are mean + S.E. of 3 different experiments. * $P<0.05$.

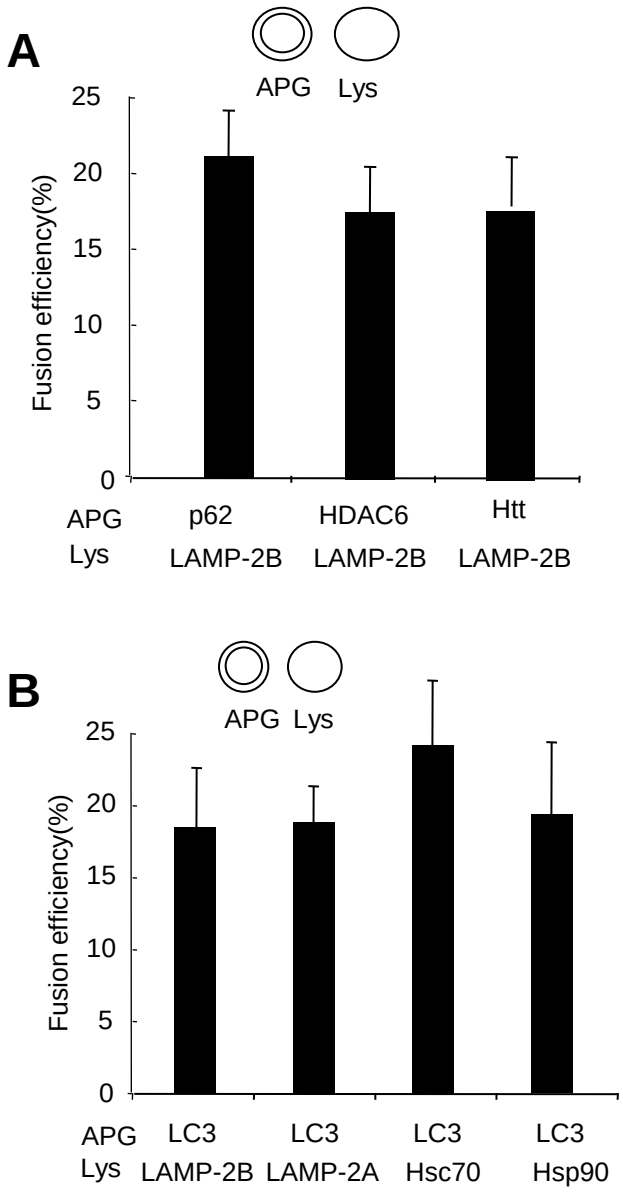

Figure S3. Effects of labeling APGs and lysosomes with different antibodies on their fusion ability. *A-B*) APGs and lysosomes isolated from mouse liver were labeled with indicated antibodies and fusion events were analyzed. Values are expressed as percentage of fusion events relative to the total number of particles in the field and are mean + S.E. of 4 different experiments.

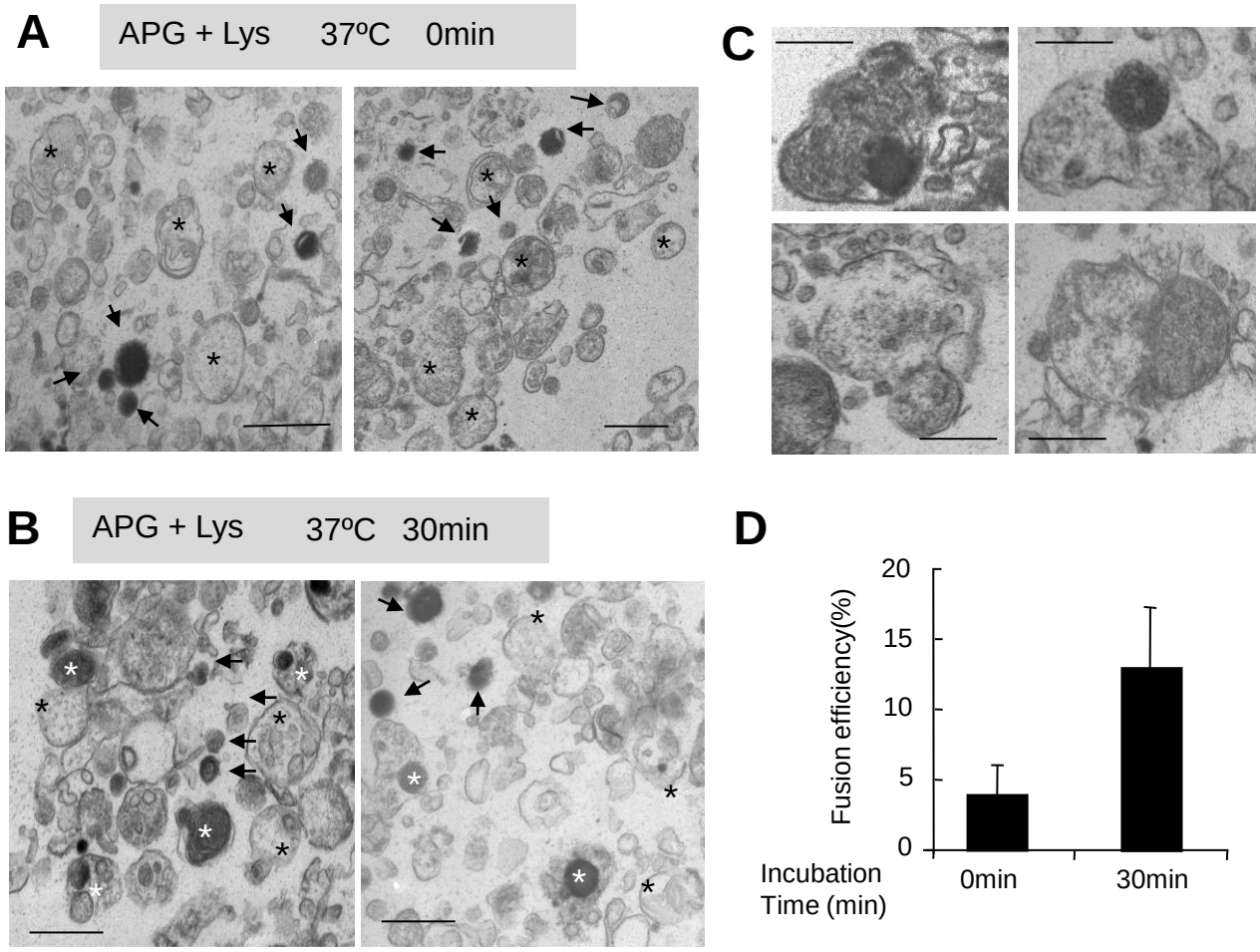

Figure S4. Ultrastructure of autophagosomes, lysosomes and their intermediate fusion compartments. *A-B*) Representative electron micrographs of the mixtures of autophagosomes (APG; black asterisk) and lysosomes (Lys; arrows) incubated in the fusion reaction at 37° C for 0 (*A*) or 30min (*B*). Fusion compartments are labeled with a white asterisk. Bar: 1μm *C*) Higher magnification images to show details of fusing compartments, identified as vesicular structures with a polarized region of higher density (Lys) within a continuous membrane. Bar: 0.2μm *D*) Quantification of the number of fusing compartments as the ones shown in *C* in organelle mixtures incubated for the indicated times. Values are expressed as percentage of total vesicles in the field and are mean + S.E. of 3 different experiments.

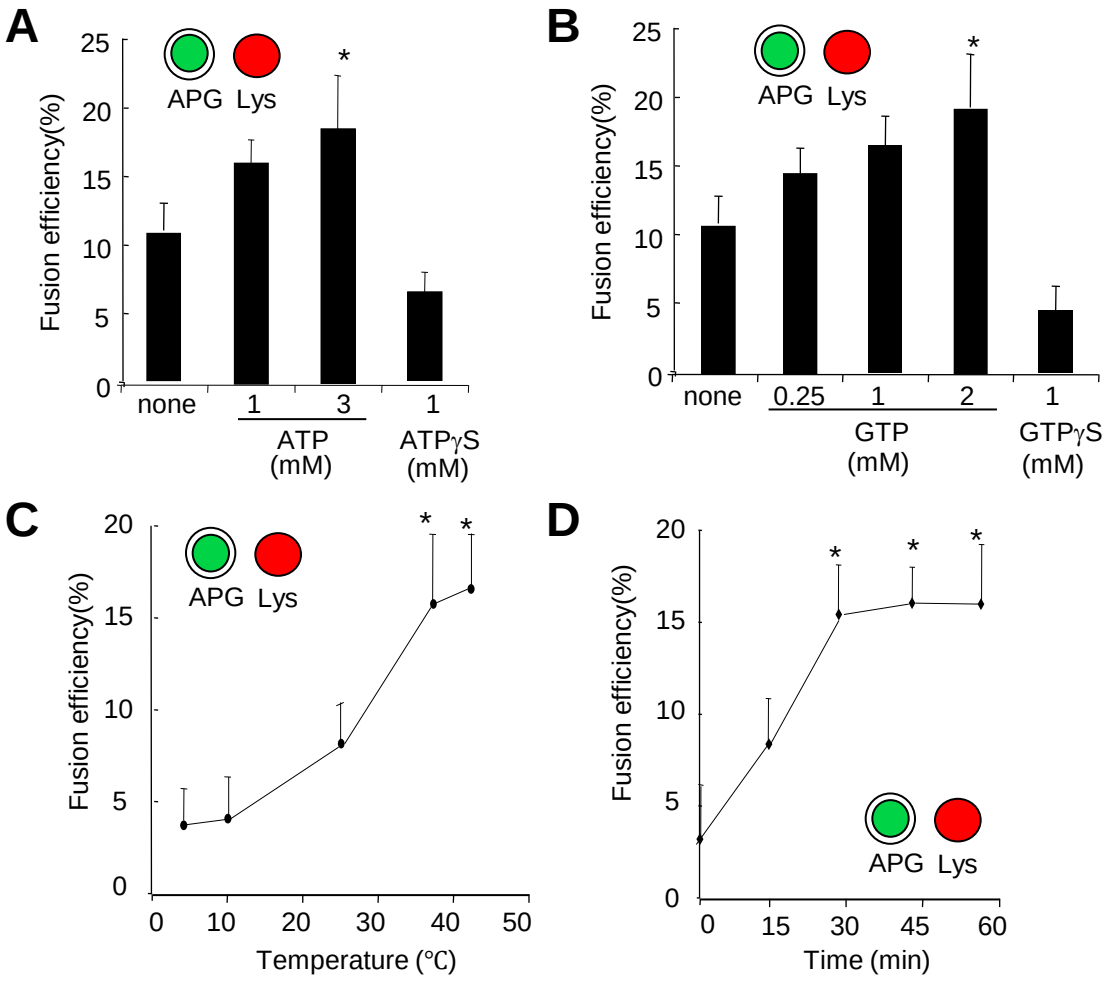

Figure S5. Requirements for heterotypic APG-lysosome fusion using a cargo mixing assay. Fusion events between APGs and lysosomes isolated from NIH-3T3 cells previously incubated with monodansylcadaverine (MDC) and with LysoTracker, respectively. *A-B)* Fusion efficiency of the organelle mixtures incubated at 37° C for 30 min in the presence of the indicated concentrations of ATP and its non-hydrolysable analog ATPγS (*A*), GTP and its non-hydrolysable analog GTPγS (*B*). *C-D)* Fusion efficiency of the organelle mixtures incubated for 30 min at the indicated temperatures *(C)* or at 37° C for the indicated periods of time *(D)*. Values are expressed as percentage of fusion events relative to the total number of particles and are means + S.E. of 3 different experiments. (* P<0.05)

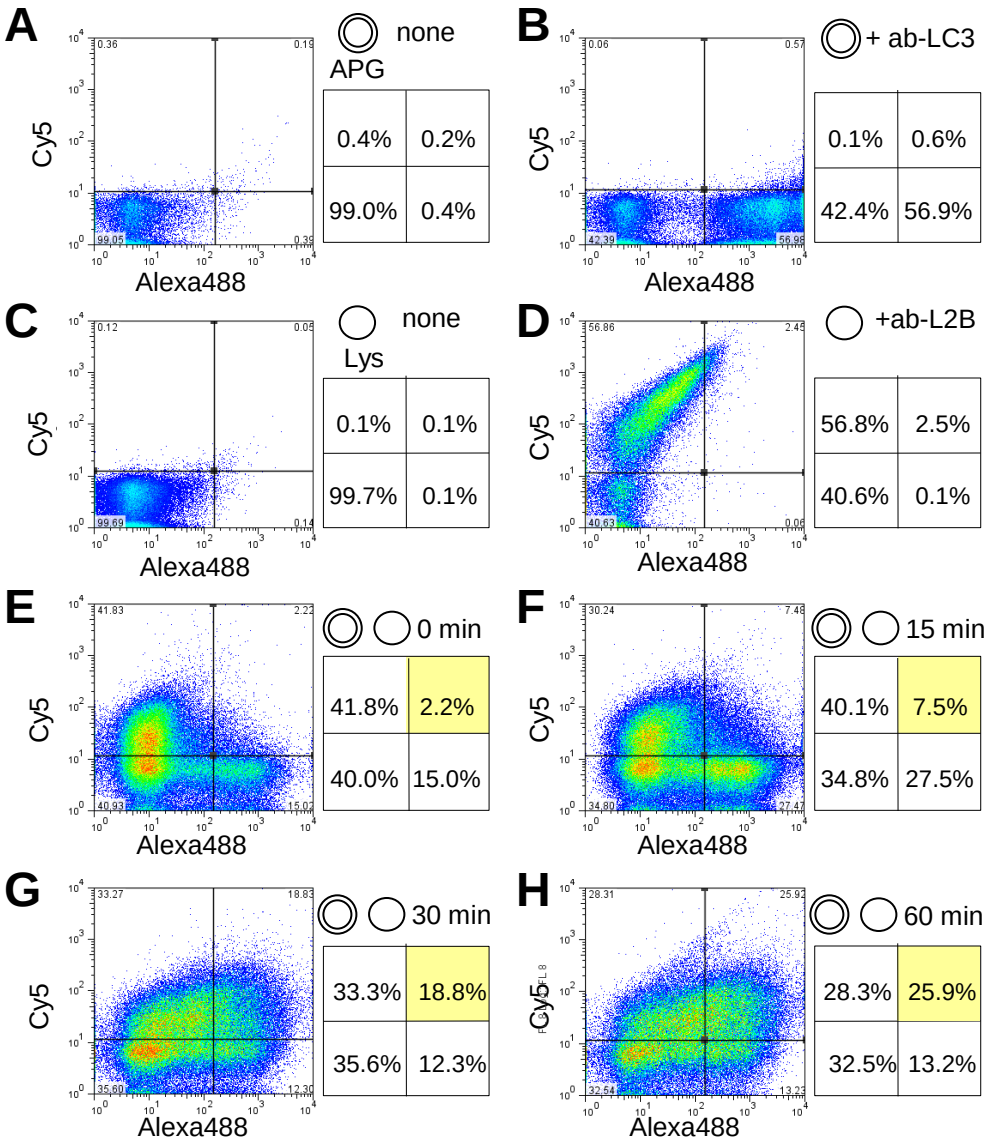

Figure S6. Analysis of the time course of APGs-lysosomes fusion using FACS analysis. *A-D*) APGs unlabeled (*A*) or labeled with anti-LC3 (*B*) and lysosomes unlabeled (*C*) or labeled with anti-LAMP-2B (*D*). *E-H*) The labeled fractions were incubated for the indicated times and then subjected to FACS analysis. Particle sorting analysis (left) and percentage of particles detected in each channel (right) are shown. Yellow regions correspond to double positive particles.

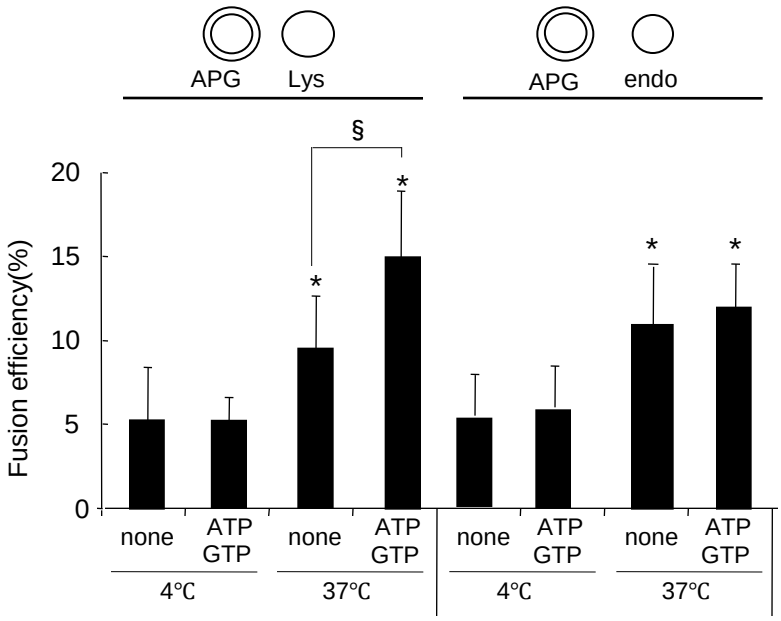

Figure S7. Effect of nucleotide supplementation in autophagosome fusion to lysosomes and endosomes at different temperatures. Autophagosomes (APGs) labeled with LC3 and FITC were incubated with LAMP-2B-labeled lysosomes (Lys) or Texas-red asialoglycoprotein receptor labeled endosomes (endo) at the indicated temperatures without additions (none) or in the presence of 1mM of the indicated nucleotides. Values are expressed as percentage of fusion events relative to the total number of particles in the field and are mean + S.E. of 3 different experiments. (*, § $P<0.05$).

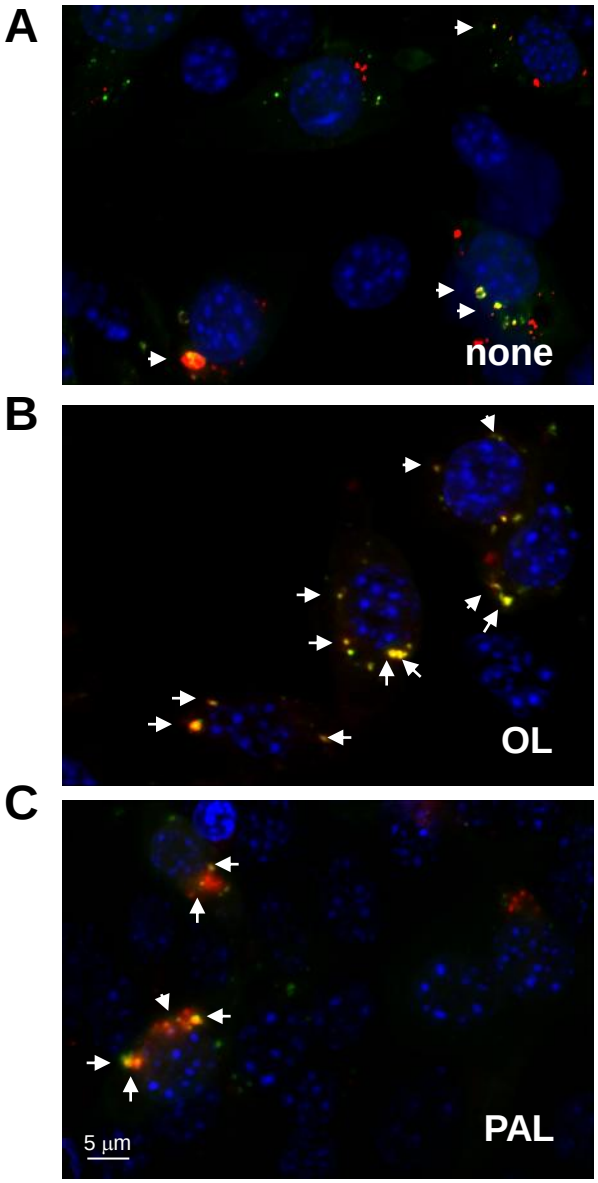

Figure S8. Autophagic fusion events change in response to lipid treatment. NIH-3T3 cells transiently transfected with the GFP-mCherry-LC3 reporter were maintained without additions (none) or treated with oleate (0.25mM) or palmitate (0.25mM) for 24 h. Arrows point to APGs (yellow) whereas autophagolysosomes are seen as red puncta.

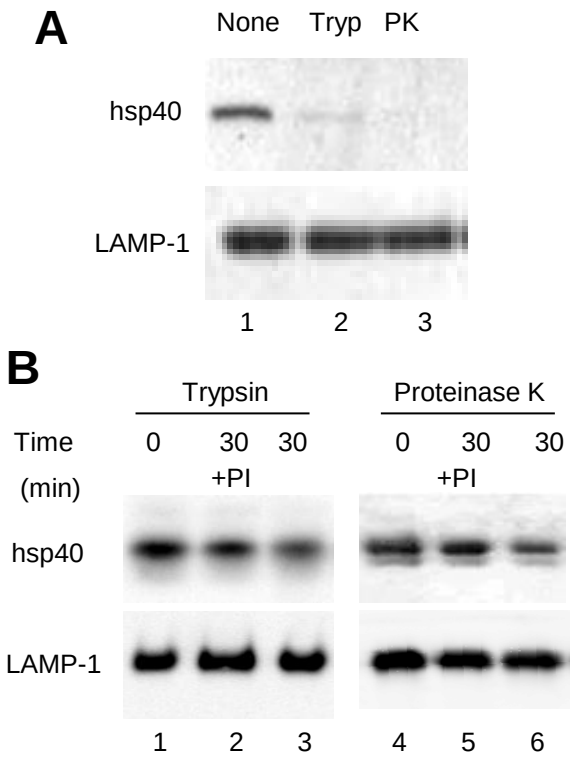

Figure S9. Efficiency of the protease treatment of isolated lysosomes. *A).* Lysosomes were treated with 10mg/ml of trypsin (Tryp) at room temperature for 15 min or with 10mg/ml of proteinase K (PK) at 4˚ C for 15 min. At the end of the incubation samples were collected and subjected to immunoblot for hsp40, a protein described to be on the cytosolic side of the lysosomal membrane and LAMP-1, with an antibody that detects its luminal region. *B)* To test the efficiency of the cocktail of protease inhibitors used to prevent further undesired digestion of the samples during the fusion assay, similar protease treatments were set but with half of the concentration of the proteases used in A. At the end of the incubation, samples were collected by centrifugation and incubated or not at 37˚ C for 30 min as labeled. Where indicated, samples were supplemented with a cocktail of protease inhibitors (+PI). All samples were processed as in A.